Catal Lett (2012) 142:1180–1189
DOI 10.1007/s10562-012-0882-5

Hydroisomerization of *n*-Hexadecane Over Anion Modified Pt/HfO_2 Catalysts

Muthu Kumaran Gnanamani · Linda Z. Linganiso · Gary Jacobs · Robert A. Keogh · Wilson D. Shafer · Burtron H. Davis

Received: 24 April 2012 / Accepted: 18 July 2012 / Published online: 14 August 2012

Abstract Pt-promoted tungsten-hafnia catalysts containing different amounts of tungsten (15 and 20 wt% WO_3) were prepared and tested for hydroisomerization of *n*-hexadecane in a trickle-bed reactor. All catalysts were calcined under dry air flow at 723 K for 3 h. Pt-promoted sulfated hafnia was also prepared for the purpose of comparison. The catalysts were characterized using BET surface area, X-ray diffraction, and DRIFTS for the adsorption of pyridine. Tungsten-based hafnia catalysts exhibit moderate activity (<80 %) for hydroisomerization of *n*-hexadecane at a higher operating temperature of 673 K compared to sulfated hafnia (>95 %), which had an operating temperature of 493 K. However, tungsten-based hafnia catalysts were more selective towards iso-C_{16} even at higher *n*-hexadecane conversions. More cracking products were obtained with sulfated hafnia in which the selectivity to iso-C_{16} decreases exponentially with *n*-hexadecane conversion. The less acidic tungsten–hafnia catalysts may be suitable for producing more isomerized products compared to the sulfated analog.

Keywords Tungstated–hafnia · Sulfated hafnia · Tungstated-zirconia · Hydroisomerization · *n*-Hexadecane · Cracking

1 Introduction

Today, the isomerization of *n*-paraffins plays an important role in the petroleum industry [1]. The most widely applied isomerization catalysts include toxic and corrosive liquid acids, such as H_2SO_4 and HF, metal halides, and metal oxides promoted with Cl or F. These reagents are highly corrosive and hence, environmentally hazardous. Many solid acids, such as zeolites, modified metal oxides, and clays, avoid these shortcomings, and offer to tune not only the number of acid sites but also their strength [2–5]. Among the solid acid catalysts studied, ZrO_2 modified by anions such as tungstate, sulfate, or phosphate, has attracted considerable attention. ZrO_2 promoted with sulfate groups was first proposed as a possible substitute by Holm and Bailey [6]. The catalyst was found to be active for the isomerization of light straight-chain alkanes at low temperatures (303–423 K). Furthermore, the stability of sulfated zirconia catalysts was improved by adding noble metals or other transition metal oxides. However, sulfated zirconia catalysts suffer from rapid loss of catalytic activity and also downstream containment and corrosion issues.

Hino and Arata [7, 8], pioneers in this field, reported that tungstated-zirconia can be used as a strong solid acid catalyst. Although tungstated-zirconia catalysts are markedly less active than sulfated zirconia, they have shown superior stability and selectivity toward the isomerization of larger alkanes such as *n*-heptane, especially when promoted with platinum [9, 10]. The reason for the appearance of strong acidity in tungstated ZrO_2 remains unclear in many cases and continues to be discussed in the literature [11–15]. Iglesia et al. [12, 15] proposed that platinum particles dissociate molecular hydrogen into hydrogen atoms which spill over to acid sites on the catalyst surface to increase *n*-alkane conversion rates and isomerization selectivities.

It is known that *n*-paraffins first undergo isomerization and then cracking [16]. The extent to which isomerization occurs depends on many factors such as the strength and amount of acid sites, the hydrogenation/dehydrogenation

M. K. Gnanamani · L. Z. Linganiso · G. Jacobs · R. A. Keogh · W. D. Shafer · B. H. Davis (✉)
Center for Applied Energy Research, University of Kentucky, 2540 Research Park Dr., Lexington, KY 40511, USA
e-mail: burtron.davis@uky.edu

activity of catalysts, the surface area and pore size distribution and also many process variables such as temperature, pressure, % conversion, H_2/*n*-paraffin ratio, etc.

Hydroisomerization of *n*-hexadecane using Pt-promoted sulfated zirconia has been studied by Wen et al. [17] and Keogh et al. [18, 19]. Due to the highly acidic nature of the catalyst, sulfated zirconia produces more cracking products even at low *n*-hexadecane conversions. Later, Zhang et al. [20, 21] investigated the performance of Pt-promoted tungstated–zirconia catalyst for the hydroisomerization of *n*-hexadecane. The authors concluded that tungstated-zirconia is highly active and selective for the hydroisomerization of long chain *n*-paraffins. Recently, Martinez et al. [22] found that the maximum isomerization activity of Pt-promoted tungstated-zirconia was obtained for the hydroisomerization of *n*-hexadecane below the monolayer coverage of WO_3. Hence, it is highly desirable to modify the strength and nature of acid sites by varying the catalytic materials that selectively produce more isomerized products. In this communication, we prepared tungstated–hafnia catalysts at two different tungsten loadings (15 and 20 wt% WO_3) by a urea hydrolysis method and promoted them with Pt (1 wt%). The prepared catalysts were tested for hydroisomerization of *n*-hexadecane in a trickle-bed reactor. The activity and selectivity of catalysts were compared between tungstated and sulfated hafnia catalytic systems.

2 Experimental

2.1 Catalyst Preparation

$Hf(OH)_4$ was obtained by the hydrolysis of hafnium chloride (Sigma-Aldrich, 99.99 % trace metals basis) in a basic ammonia solution. The precipitate was then filtered and washed with distilled water until the filtrate was free of chloride ions and finally dried in an oven at 383 K for 24 h. The tungstated–hafnia samples [HfO_2–$WO_3(X)$, $X = 15$ and 20 wt%] were prepared by incipient wetness impregnation (IWI) of $Hf(OH)_4$ using a solution of ammonium metatungstate (Sigma-Aldrich, ≥99.0 % WO_3 basis) of an adequate concentration in order to obtain two different WO_3 contents on the final catalyst (15 and 20 wt%). After impregnation, the solid was dried in an oven at 383 K overnight and calcined in air (50 ml min^{-1}) at 1,123 K for 3 h. The calcined $WO_3(X)$–HfO_2 catalysts were promoted with 1 wt% Pt using IWI of an aqueous tetraammineplatinum(II) chloride hydrate solution (Aldrich Chem Co. 98 %). Then, the catalysts were dried at 383 K overnight and calcined in air at 723 K for 3 h. For the purpose of comparison, 1 % Pt-promoted $WO_3(15)$–ZrO_2 catalyst was also prepared by following a similar method as described above.

The sulfated hafnia sample was obtained by immersing hafnium hydroxide gel in 1 N H_2SO_4 [10 ml/g of $Hf(OH)_4$]. The slurry was stirred at room temperature for 1 h, after which the solid was filtered without further washing. The obtained solid was dried at 393 K for 5 h prior to impregnation with Pt (1 wt%). The chemical analysis of this catalyst indicated a content of 2.46 wt% S. All the catalyst samples prepared were kept in a glove box under helium atmosphere prior to characterization and activity testing.

2.2 Catalyst Characterization

2.2.1 X-Ray Diffraction

XRD measurements were carried out using a Philips X'Pert diffractometer with monochromatic Cu Kα radiation ($\lambda = 1.5418$). XRD scans were taken over a range of 2θ from 10 to 90°. The scanning step was 0.01, the scan speed was 0.0025 s^{-1}, and the scan time was 4 s. Peaks located at $2\theta = 28.6$ and 31.9° are attributed to the monoclinic phase of hafnia and those located at $2\theta = 30°$ to the tetragonal phase. The peaks located at $2\theta = 23$–25° are assigned to WO_3.

2.2.2 N_2 Physisorption

The specific surface areas (BET) of the catalysts were obtained from nitrogen adsorption isotherms at 77 K by using a Micromeritics Tri-Star gas adsorption system. The samples were previously pretreated at 623 K overnight under vacuum (10^{-5} Torr).

2.2.3 DRIFT Spectroscopy with Pyridine Adsorption

Diffuse reflectance infrared Fourier transform (DRIFT) spectroscopy was employed to study pyridine adsorption on acidic sites of the catalysts. For measurement of IR spectra, catalyst powder placed in an in situ IR cell was pretreated with helium at 773 K for 2 h, and reduced under flowing hydrogen at 473 K for another 2 h. The samples were cooled to 323 K under helium and subsequently exposed to pyridine for 15 min by diverting the helium flow through a pyridine saturator. Spectra were then taken at 373, 473, 573, 623, and 673 K after 10 min in flowing helium at each temperature. Each spectrum was obtained by averaging 128 scans taken over the range 400–4,000 cm^{-1} at a resolution of 2 cm^{-1}.

2.3 Catalytic Test

A trickle-bed reactor was used to test the hydroisomerization activity of *n*-hexadecane for various catalysts

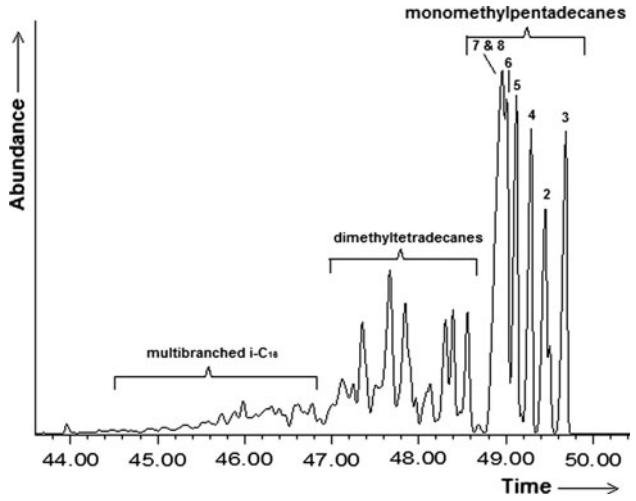

Fig. 1 A typical GC–MS spectrum of hexadecane isomers in the products of n-C_{16} hydroisomerization over Pt-promoted WO_3/HfO_2 catalysts

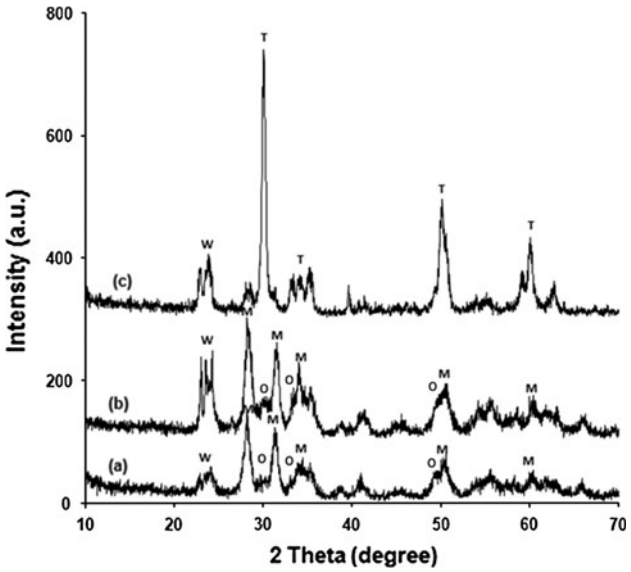

Fig. 2 XRD profiles of Pt-promoted *a* $15WO_3/HfO_2$, *b* $20WO_3/HfO_2$, and *c* $15WO_3/ZrO_2$ catalysts (*W* tetragonal WO_3, *M* monoclinic HfO_2 or ZrO_2, *T* tetragonal HfO_2 or ZrO_2, *O* orthorhombic HfO_2 or ZrO_2)

(Fig. 1). Reaction temperatures were controlled by a temperature controller (Omega ramp and soak programmable temperature controller, controlled to ±1 K), and system pressures were set using a back-pressure regulator. *n*-Hexadecane (99 wt% Sigma-Aldrich) was delivered by a syringe pump at different rates in order to test the catalyst at different conversion levels. Each experimental condition was maintained for 15–20 h before switching to another condition. Using nitrogen inert gas, the total gas flow rate was kept constant (hydrogen + nitrogen) when studying conversion effects of hexadecane, and the flow rates of hydrogen and nitrogen gases were maintained by separate mass-flow controllers.

Typically 2.5 g of calcined catalyst (40–100 mesh) were loaded into the reactor after mixing with an equivalent weight percentage of powdered glass beads (100 mesh). Before measuring the catalytic activity, all samples were pretreated in situ in the reactor. First, the catalyst was purged under nitrogen flow (50 sccm) at 673 K for 3 h, and then reduced under hydrogen flow (50 sccm) at 473 K for 2 h. The reactor was then pressurized to 2.16 MPa and a hydrogen flow rate was established using the mass-flow controller to obtain a hydrogen to *n*-hexadecane molar feed ratio of 2.0. Each catalyst was tested for isomerization activity of *n*-hexadecane by following two sets of conditions. In one case, the WHSV of *n*-hexadecane was varied by keeping the amount of catalyst constant, while the feed rate of *n*-hexadecane was varied. In another run, the H_2/*n*-hexadecane was varied while maintaining the WHSV and the amount of catalyst constant. The effluent gases were analyzed online using a Micro GC (HP, Quad series, Refinery Gas analyzer) equipped with a TCD detector. Liquid products were collected in a trap maintained at room temperature (298 K) for analysis using a 60 m × 0.32 mm DB-5 capillary column (0.25 μm thickness) installed in a HP 7890 GC chromatograph. A 5973 N MSD coupled to the 6890 GC from Agilent was employed for identification of various hydrocarbons and quantified using a FID detector. A part of the GC–MS pattern (i.e., the peaks corresponding to isomers of n-C_{16} obtained from hydroisomerization of *n*-hexadecane) is shown in Fig. 2. Each peak in the methyl pentadecane region was identified and marked whereas dimethyl tetradecanes and multibranched components were not able to be separated and identified individually with our available GC techniques.

3 Results and Discussion

The textural characterization data for unpromoted and Pt-promoted catalysts are shown in Table 1. The BET surface areas of the catalysts were found to decrease with increasing WO_3 content on hafnia; however, considering the added weight of WO_3 the surface area is essentially the same, suggesting that the WO_3 is essentially a monolayer structure. By addition of tungsten to ZrO_2 (15 and 20 wt%), the total pore volume of the catalyst decreased. However, regarding the mean pore radii of the catalysts, for 15 %WO_3/HfO_2 it decreased from 4.67 to 4.49 nm, whereas for 20 %WO_3/HfO_2 it exhibited slightly higher mean pore radii of 5.61 nm as compared to hafnia. At equivalent W loading, the WO_3/ZrO_2 catalyst exhibits a higher surface area compared to the WO_3/HfO_2 catalyst. This is due to the fact that the surface area of ZrO_2 is higher than HfO_2 under our preparation conditions. All W-containing catalysts were calcined in air at 1,123 K;

Table 1 Textural and compositional properties of the samples

Sample	WO_3 (wt%)	Pt (wt%)	S_{BET} (m^2/g)	Total pore volume (cm^3/g)	Average pore radius (nm)
HfO_2	0	0	30.0	0.102	4.67
$15WO_3/HfO_2$	15.0	0	23.3	0.050	4.49
$20WO_3/HfO_2$	20.0	0	20.8	0.055	5.61
$1Pt–15WO_3/HfO_2$	14.85	1.0	24.2	0.049	4.26
$1Pt–20WO_3/HfO_2$	19.80	1.0	21.0	0.054	5.40
$1Pt–15WO_3/ZrO_2$	14.85	1.0	47.2	0.057	2.52

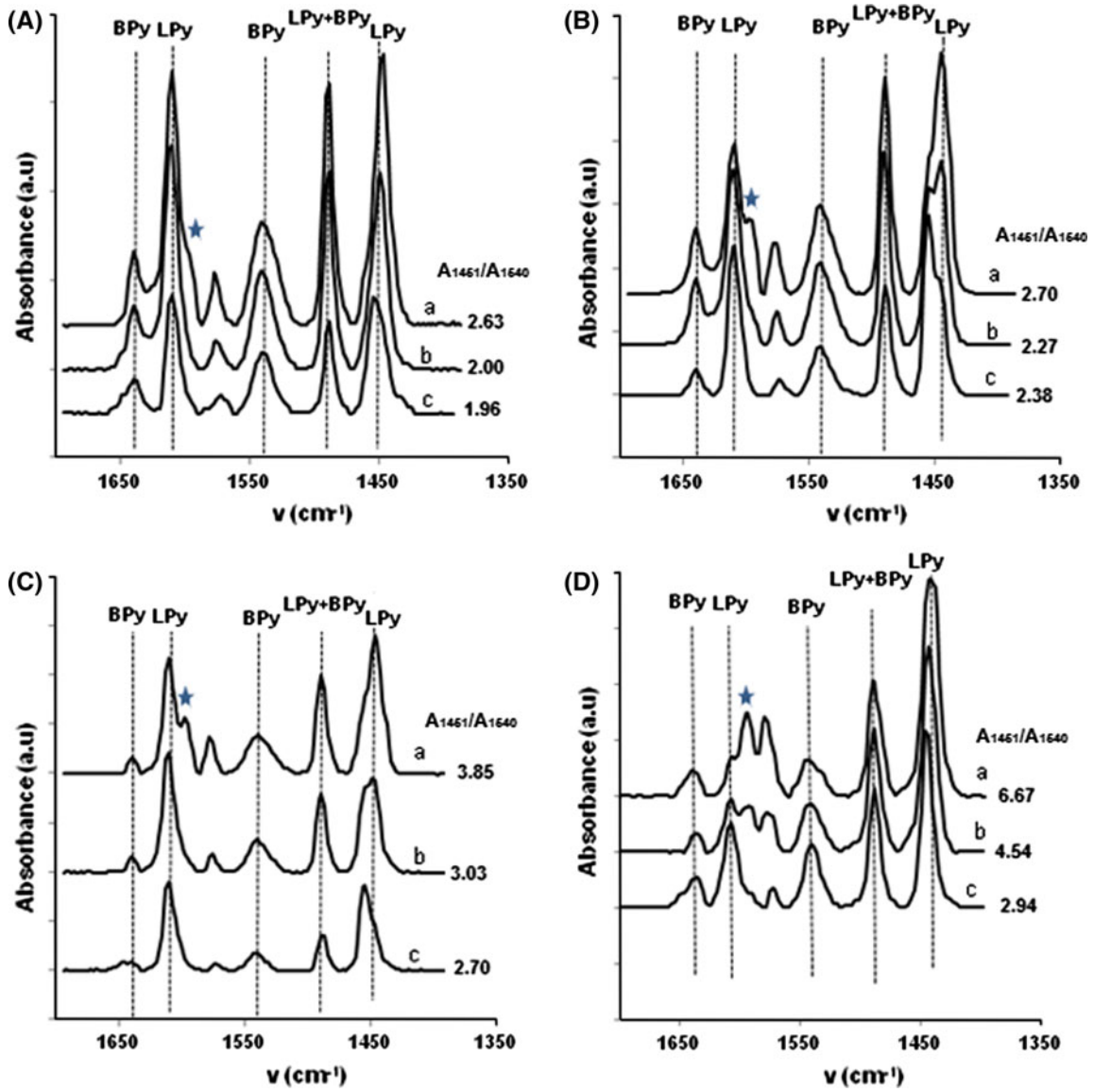

Fig. 3 DRIFT spectra for pyridine desorption at various temperatures (*a* 323 K; *b* 373 K; *c* 473 K) for **A** $1Pt15WO_3/HfO_2$, **B** $1Pt20WO_3/HfO_2$, **C** $1Pt15WO_3/ZrO_2$, **D** $1Pt/HfO_2–SO_4$ catalysts (★ absorption corresponds to physically adsorbed pyridine) [A_{1451}/A_{1540} refers to the L/B acid ratio]

thus, it is reasonable to expect such lower values for surface area (e.g., 30–50 m^2/g).

The identification of hafnia, zirconia and tungsten oxide phases was made using X-ray diffraction. Figure 2 displays the X-ray diffraction patterns for HfO_2 and ZrO_2 containing catalyst samples. The pattern for zirconia shows several crystalline peaks corresponding to both monoclinic and tetragonal phases of zirconia; in addition, tungstate in the

form of the tetragonal phase is also present. The zirconia is present predominantly in the tetragonal form. At ambient conditions, HfO_2 has a monoclinic baddeleyite structure (space group $P21/c$) with 2° in the range of 27.5–29.5° and this transforms to the orthorhombic structure at high temperatures and pressures [23]. The emergence of crystalline WO_3 with increasing tungsten loading on HfO_2 was identified by three peaks in the X-ray diffraction pattern in the 2° range of 23–25°. In other words, the nature of the phase existing on a working catalyst might be different for zirconia and hafnia containing catalysts.

The acidic properties of the catalysts were studied to identify the relationship between catalytic activity and acidity. DRIFT spectroscopy with pyridine adsorption was used to determine (i) the nature of the acid sites (i.e. Brønsted or Lewis acid sites) and (ii) the relative strengths of various tungstated–hafnia and tungstated zirconia catalysts. Figure 3 shows the DRIFT spectra of adsorbed pyridine on H_2 pretreated hafnia and zirconia based catalyst samples. Based on the available literature, it is possible to identify the observed IR absorbance bands after desorbing pyridine at temperatures in the range of 323–473 K. The characteristic bands at 1640, 1607, 1540 and 1490 cm^{-1} are assigned to pyridinium ions adsorbed on Brønsted acid sites [24]. The bands at 1610, 1575, 1490, and 1447 cm^{-1} correspond to pyridine adsorbed on Lewis acid sites. The acid sites on the surface of catalyst may be quantified by calculating the L/B acid ratio. This ratio may be determined using the IR peak intensities of the pyridine-lewis acid site complex at 1,451 cm^{-1} and the pyridine-Brønsted acid site complex at 1,540 cm^{-1}. Irrespective of catalyst, the L/B ratio decreased with pyridine desorption temperature. The sulfated hafnia ($1Pt/HfO_2–SO_4$) and tungstated–zirconia ($1Pt–15WO_3/ZrO_2$) catalysts exhibited a much higher Lewis acid site density as compared to tungsten-containing hafnia catalysts ($1Pt–15WO_3/HfO_2$ and $1Pt–20WO_3/HfO_2$). The reason for the appearance of strong acidity in tungsten-containing ZrO_2 remains under debate and continues to be discussed in the literature [11–15]. Many have assumed that the super acidity of WO_3/ZrO_2 must be associated, as in the case of SO_4^{2-}/ZrO_2, with the formation of strong Lewis centers. Likewise, tungsten-containing hafnia should also display similar phenomena due to the position of Hf in the periodic table. Arata et al. [25] found that the addition of sulfate ion to HfO_2 promotes acidity that catalyzes the isomerization of butane to isobutane. Recently, Ahmed et al. [26] reported that the addition of small amounts of hafnia stabilizes the surface sulfate complex, the tetragonal phase of zirconia, and enhances their activity for the isomerization of butane to iso-butane. In this study, Fig. 3 displays significant evidence for bands corresponding to Brønsted and Lewis acid sites upon desorption of pyridine even at 473 K on

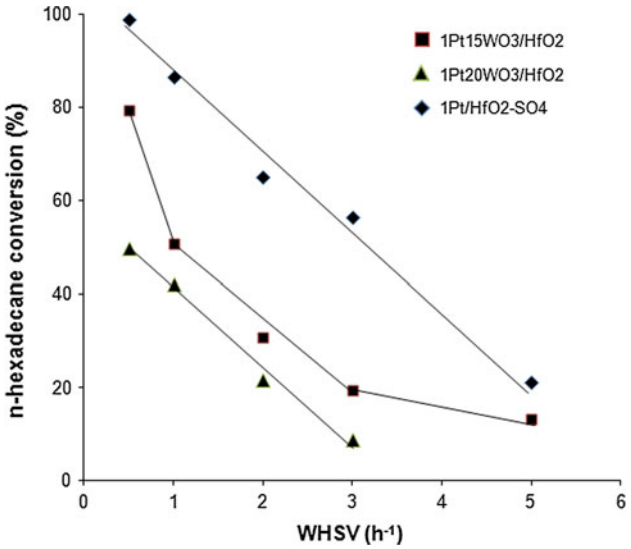

Fig. 4 Conversion of *n*-hexadecane as a function of WHSV over various HfO_2 based catalysts (reaction condition: $1Pt(X)WO_3/HfO_2$ = *T* 573 K, *P* 2.16 MPa, H_2/*n*-hexadecane = 2.0; $1Pt/HfO_2–SO_4$ = *T* 483 K, *P* 2.16 MPa, H_2/*n*-hexadecane = 2.0)

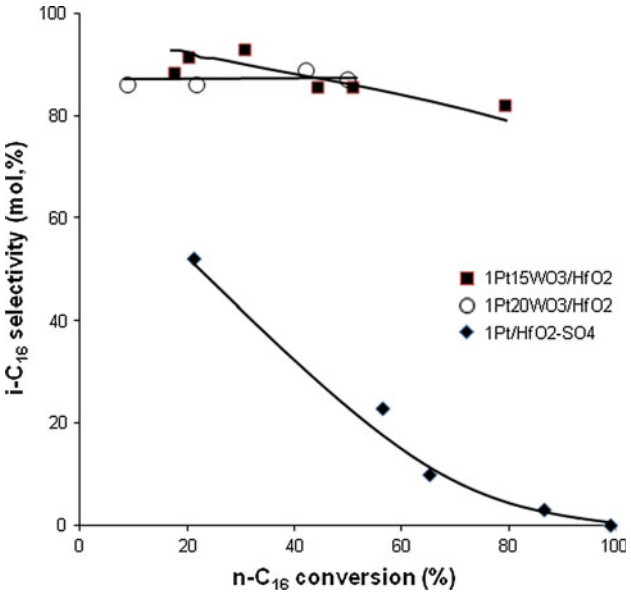

Fig. 5 i-C_{16} selectivity as a function of *n*-hexadecane conversion over various HfO_2 based catalysts (reaction condition: $1Pt(X)WO_3/HfO_2$ = *T* 573 K, *P* 2.16 MPa, WHSV = 0.5–5.0 h^{-1}, H_2/*n*-hexadecane = 2.0; $1Pt/HfO_2–SO_4$ = *T* 483 K, *P* 2.16 MPa, WHSV = 0.5–5.0 h^{-1}, H_2/*n*-hexadecane = 2.0)

tungsten- and sulfate-containing hafnia catalysts. A detailed correlation between acidity and catalytic activity will be discussed.

Figure 4 shows a comparison graph of n-C_{16} conversion with WHSV for various HfO_2 catalysts. Irrespective of catalyst type, conversion of *n*-hexadecane increased by decreasing the space velocity of the reactant. Sulfated hafnia ($1Pt/HfO_2–SO_4^{2-}$) catalyst displayed higher activity

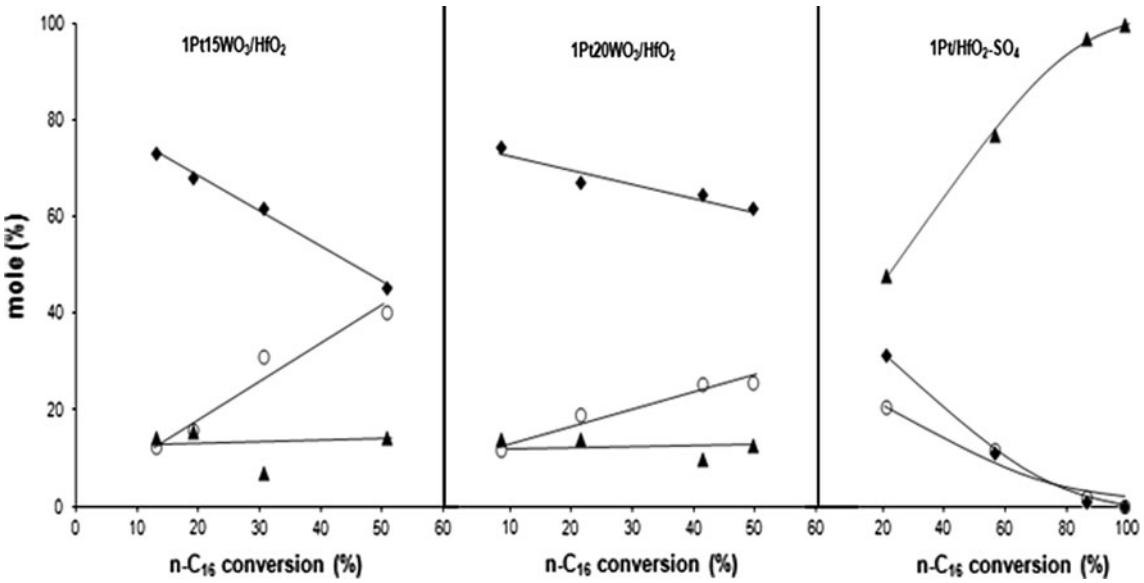

Fig. 6 Relative distribution of mono and multi-branched *i*-C_{16} for hydroisomerization of *n*-hexadecane over various HfO_2 based catalysts (reaction condition: 1Pt(X)WO_3/HfO_2 = *T* 573 K, *P* 2.16 MPa, WHSV = 0.5–5.0 h^{-1}, H_2/*n*-hexadecane = 2.0; 1Pt/HfO_2–SO_4 = *T* 483 K, *P* 2.16 MPa, WHSV = 0.5–5.0 h^{-1}, H_2/*n*-hexadecane = 2.0) (◆ mono-branched, ○ multi-branched, ▲ cracking products)

Table 2 Comparison of hydroisomerization activity of *n*-hexadecane

Catalysts	1 %Pt–15 % WO_3/HfO_2[a]	1 %Pt–20 % WO_3/HfO_2[a]	1 %Pt–15 % WO_3/ZrO_2[b]	1 %Pt/HfO_2–SO_4[c]
n-C_{16} conversion (%)	79.3	49.7	84	65.0
Isomerization (%)	82.1	87.3	45.6	9.9
Cracking (%)	17.9	12.7	54.4	90.1
i-C_{16} distribution (%)				
Mono-branched	62.5	70.7	32.8	52.7
Multi-branched	37.5	29.3	67.2	47.3
Distribution of mono-branched isomers (%)				
7 + 8Me–C_{15}	28.8	28.2	27.4	26.2
6Me–C_{15}	13.9	14.9	14.0	13.3
5Me–C_{15}	14.9	15.0	14.9	14.4
4Me–C_{15}	13.7	13.8	13.1	13.7
2Me–C_{15}	11.1	10.5	12.8	11.8
Et–C_{14}	2.8	2.5	2.4	3.2
3Me–C_{15}	14.8	15.0	15.2	17.5

Reaction conditions: [a] *T* 573 K, *P* 2.16 MPa, WHSV = 0.5 h^{-1}, H_2/*n*-hexadecane = 2.0; [b] *T* 503 K, *P* 2.16 MPa, WHSV = 1.0 h^{-1}, H_2/*n*-hexadecane = 2.0; [c] *T* 483 K, *P* 2.16 MPa, WHSV = 2.0, H_2/hexadecane = 2.0

for hydroisomerization of *n*-hexadecane compared to tungstated–hafnia catalysts (1Pt–15WO_3/HfO_2 and 1Pt–20WO_3/HfO_2) at similar residence times (WHSV). Recall that the operating temperature for the two catalytic systems is different. Among the two tungstated–hafnia catalysts, 1Pt–15WO_3/HfO_2 catalyst exhibited higher *n*-C_{16} conversion compared to the higher W loaded catalyst. However, the two W catalysts exhibited similar conversions at lower conversion levels and a more detailed assessment of the two catalysts will require a major effort.

It is known for hydroisomerization of higher alkanes over bi-functional catalysts that depending on the catalyst and reaction conditions, cracking products contribute to a considerable extent compared to the desired isomerized products. While we are not able to identify all of the branched C_{16} isomers, the GC separation allows for a definition of the amount of *i*-C_{16} formed and a grouping of the mono- and di-methyl branching as well as multi-branching (Fig. 1). In this regard, *i*-C_{16} selectivity was plotted against *n*-C_{16} conversion for various Pt-promoted hafnia catalysts as shown in Fig. 5. The tungstated–hafnia catalysts exhibited higher selectivity (>80 %) for *i*-C_{16} compared to sulfated hafnia (<50 %) of similar hexadecane conversion. As noted from Fig. 5, the selectivity to

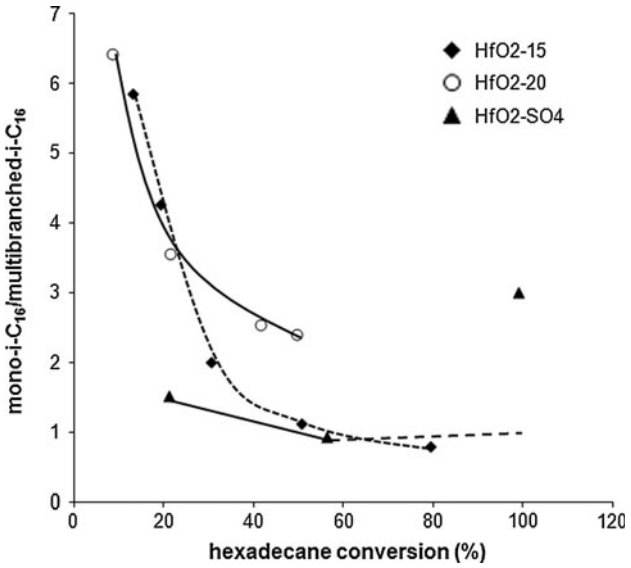

Fig. 7 Effect of *n*-hexadecane conversion on mono/multi-*i*-C_{16} ratio for hydroisomerization of *n*-hexadecane over various HfO_2 based catalysts (reaction condition: 1Pt(X)WO_3/HfO_2 = *T* 573 K, *P* 2.16 MPa, WHSV = 0.5–5.0 h^{-1}, H_2/*n*-hexadecane = 2.0; 1Pt/HfO_2–SO_4 = *T* 483 K, *P* 2.16 MPa, WHSV = 0.5–5.0 h^{-1}, H_2/*n*-hexadecane = 2.0)

i-C_{16} for tungsten catalysts remained more or less constant up to 80 % *n*-C_{16} conversion level. On the other hand, for sulfated hafnia, while exhibiting a much higher activity compared to tungstated–hafnia, selectivity towards iso-C_{16} was low and dropped from 52 to <10 % with increasing *n*-hexadecane conversion.

The product distributions obtained from hydroisomerization of *n*-hexadecane using various hafnia catalysts are shown in Fig. 6 and Table 2. The mole percents of mono-branched *i*-C_{16} for tungstated–hafnia catalysts decrease slowly with increasing *n*-C_{16} conversion; in parallel, multi-branched *i*-C_{16} products increased with increasing *n*-C_{16} conversion. Both 15 and 20 wt% WO_3 loaded Pt/hafnia catalysts display nearly constant cracking/isomerization selectivity with increasing conversion of *n*-C_{16}. However, the trend looks different on 1Pt/HfO_2–SO_4 catalyst, in which, both mono and multi-branched *i*-C_{16} drops continuously with *n*-hexadecane conversion. Also, the cracking product observed even at low *n*-hexadecane conversion was much higher than the tungsten–hafnia catalysts (>40 %).

For tungstated–hafnia catalysts, mono-branched *i*-C_{16} isomer formation is more favorable at low *n*-hexadecane conversion levels. With an increase in C_{16} conversion, mono-branched *i*-C_{16} compounds isomerized to form multi-branched isomers. It is evident from Fig. 7 that the highly acidic nature of sulfated hafnia gives more multi-branched *i*-C_{16} compared to tungstated–hafnia. It appears that the product shift from isomerization to cracking probably occurs through the inter-conversion of mono-to-multi-branched isomers by an alkyl shift mechanism. Wender et al. [21] have remarked that the multi-branched isomers can be easily cracked using Pt-promoted tungstated-zirconia catalysts since the possibility of β-scission increases when there are more tertiary carbon atoms in isomers. In our case, we observed an intermediate value of

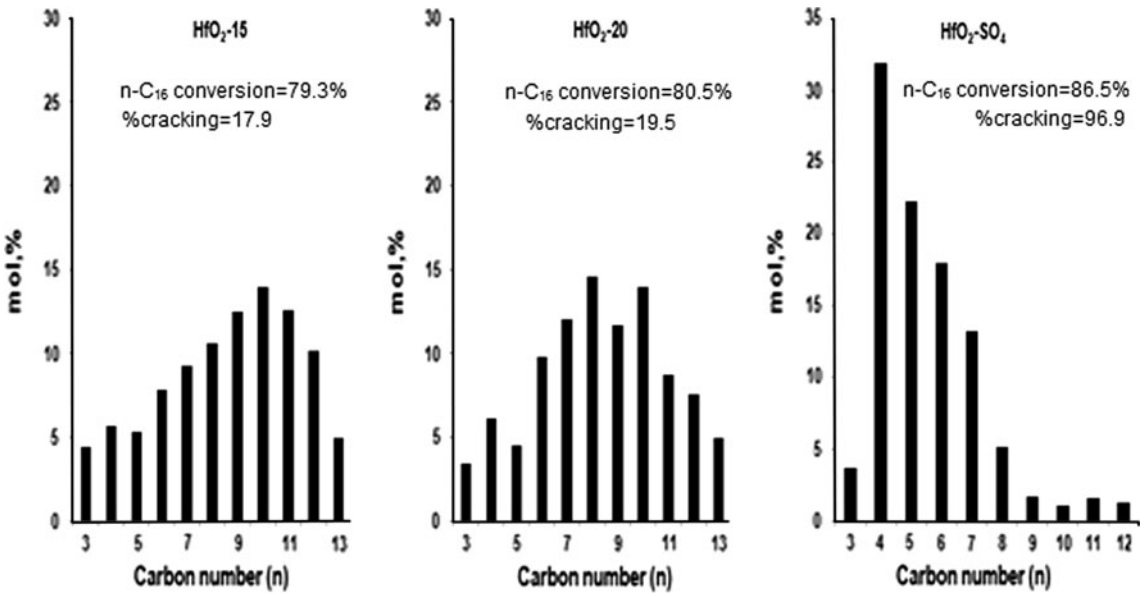

Fig. 8 Distribution of hydrocarbons obtained (except C_{16}) for hydroisomerization of *n*-hexadecane using various HfO_2 based catalysts (reaction condition: 1Pt15WO_3/HfO_2 = *T* 573 K, *P* 2.16 MPa, WHSV = 0.5 h^{-1}, H_2/*n*-hexadecane 2.0; 1Pt20WO_3/HfO_2 = *T* 573 K, *P* 2.16 MPa, WHSV = 0.2 h^{-1}, H_2/*n*-hexadecane = 2.0; 1Pt/HfO_2–SO_4 = *T* 483 K, *P* 2.16 MPa, WHSV = 1.0 h^{-1}, H_2/*n*-hexadecane = 2.0)

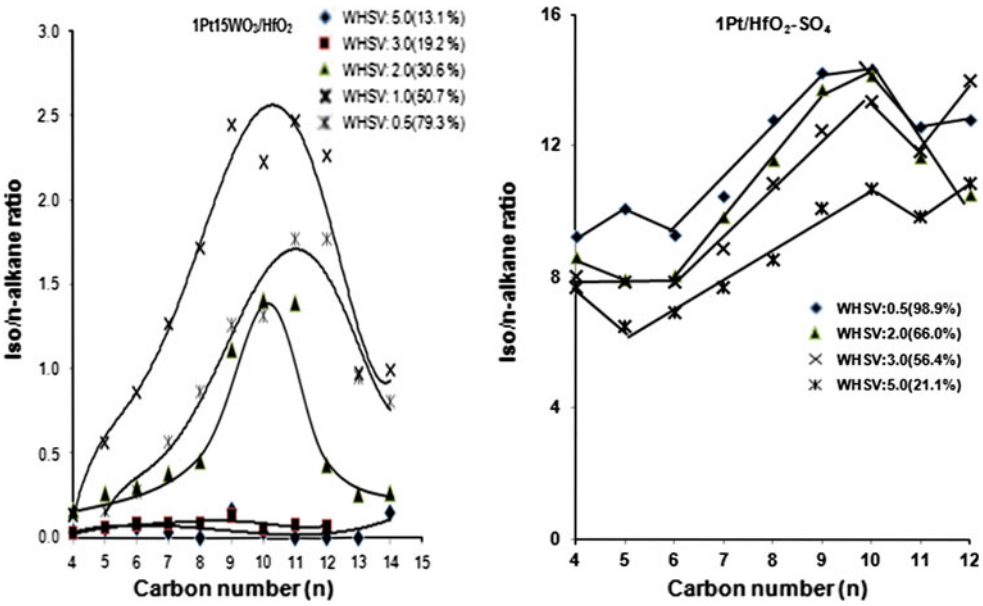

Fig. 9 Comparison of iso/*n*-alkane ratio of various carbon numbers between tungstate and sulfate modified HfO_2 catalysts for hydroisomerization of *n*-hexadecane (reaction condition: $1Pt15WO_3/HfO_2$ = *T* 573 K, *P* 2.16 MPa, WHSV = 0.5–5.0 h^{-1}, H_2/*n*-hexadecane = 2.0; $1Pt/HfO_2$–SO_4 = *T* 483 K, *P* 2.16 MPa, WHSV = 0.5–5.0 h^{-1}, H_2/*n*-hexadecane = 2.0). The *value in the parentheses* stands for % *n*-hexadecane conversion

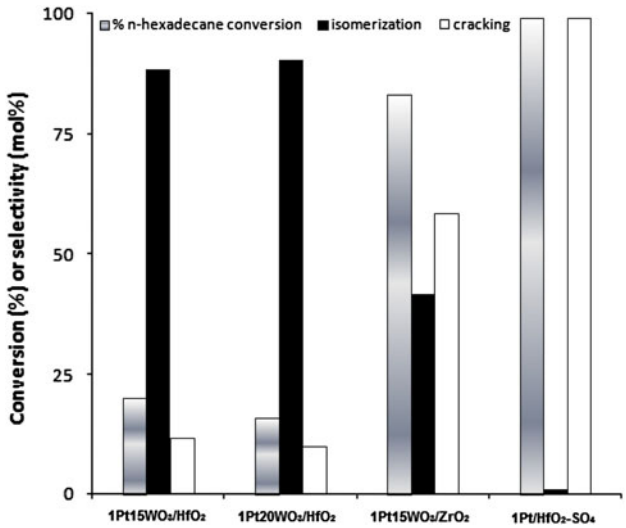

Fig. 10 Comparison of *n*-hexadecane conversion and selectivity of $1Pt(X)WO_3/HfO_2$, and $1Pt15WO_3/ZrO_2$ catalysts for hydroisomerization of *n*-hexadecane under similar reaction conditions [*T* 503 K, *P* 2.16 MPa, WHSV = 1.0 h^{-1}, H_2/*n*-hexadecane = 2.0]

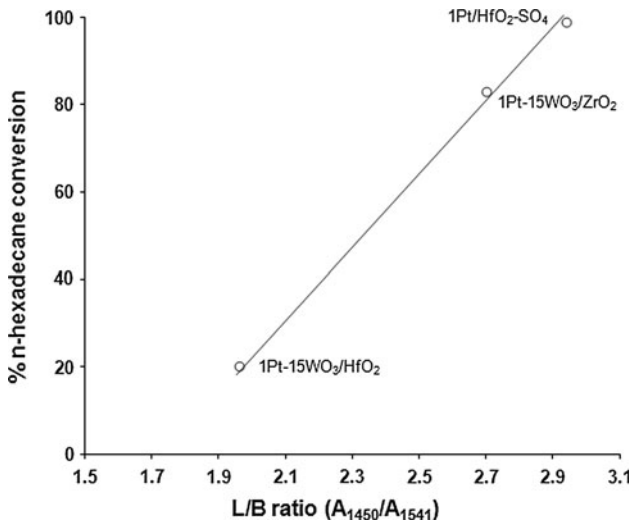

Fig. 11 Comparison of L/B ratios with *n*-hexadecane conversion for $1Pt15WO_3/HfO_2$, $1Pt15WO_3/ZrO_2$ and $1Pt/HfO_2$–SO_4 catalysts (pyridine desorption temperature was 473 K; reaction conditions: *T* = 473 K, *P* = 2.16 MPa, WHSV = 1.0 h^{-1}, H_2/*n*-hexadecane = 2.0]

mono/multi-branched *i*-C_{16} isomers (3.0–1.0) for tungstated–hafnia system over a broad range in *n*-hexadecane conversion levels (although an exception occurs at lower conversion). This could probably suppress the formation of cracking products over tungsten–hafnia catalysts. In contrast, sulfated hafnia exhibited a very similar mono/multi-branched *i*-C_{16} ratio as tungstated–hafnia, but the latter exhibited remarkably high cracking activity. Hence, it may be possible that different mechanisms are operating under our reaction conditions for cracking using tungsten and sulfated hafnia systems. Hence, irrespective of conversion level and mono/multi-branched *i*-C_{16} ratios, Pt-promoted sulfated hafnia favors more cracking than isomerization.

The distributions of lower hydrocarbons obtained through cracking of *n*-hexadecane at similar conversions over three hafnia catalysts are shown in Fig. 8. The product distribution patterns are different for tungsten and sulfated hafnia catalysts. The maximum appears at ca. C_8–C_{10} with a symmetrical distribution for 15 and 20 wt% WO_3 over hafnia catalysts. For sulfated zirconia, the cracking products peak at C_4 and the pattern indicates that the products are the result of secondary cracking reactions.

In Fig. 9 more detailed information is presented concerning the nature of cracked products at various *n*-hexadecane conversions. Iso/*n*-alkane ratio as high as 14 was obtained using sulfated hafnia catalysts and the ratio

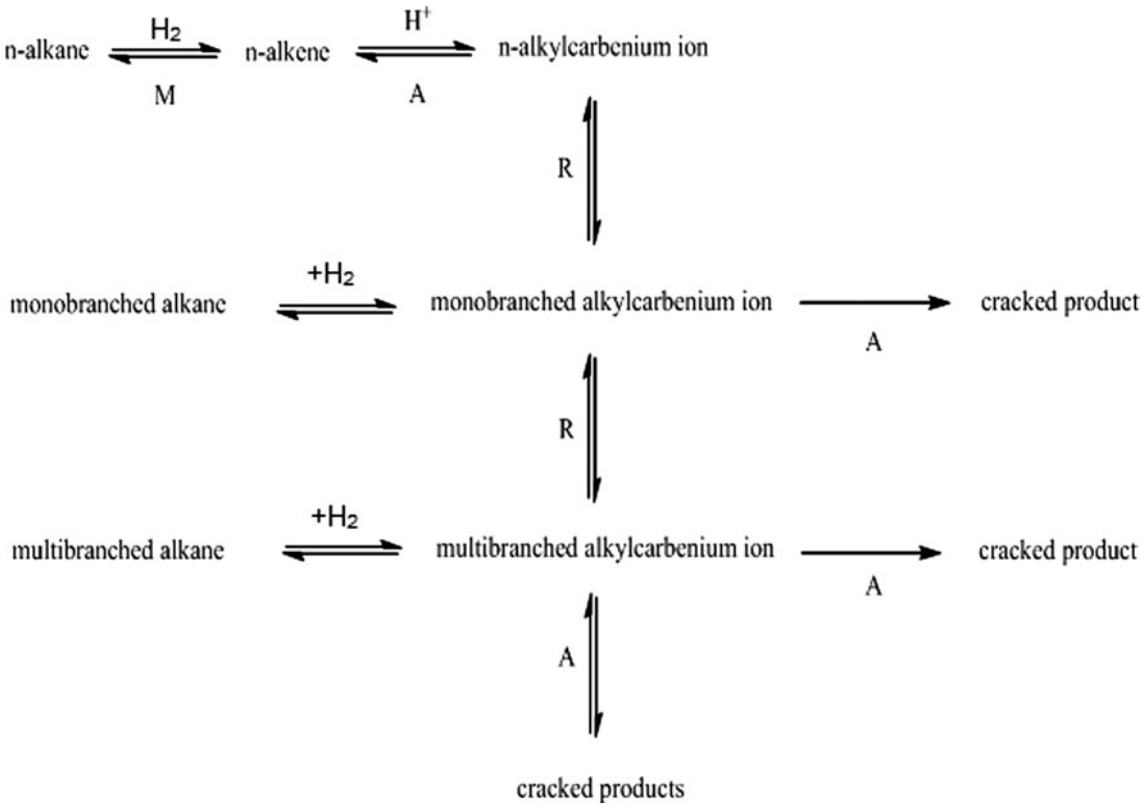

Scheme 1 Bifunctional pathways of hydroisomerization and cracking of *n*-paraffins (*M* metal sites, *A* acid sites, *R* rearrangement of carbenium ions) [33]

increases with increasing *n*-hexadecane conversion. The ratios show that secondary reactions are involved in order to produce these high *i*/*n* values. However, approximately equal amounts of *i*- to *n*-alkanes were obtained for 15 %WO_3/HfO_2 at low conversions and a maximum value of about 2.5 was obtained at high conversions. This suggests that the desorption of cracked products occurs more readily with the WO_3–HfO_2 catalyst and that primary cracked products are obtained. For sulfated HfO_2, it appears that the primary products remain adsorbed to undergo secondary cracking reactions which lead to more *i*-products.

Figure 10 illustrates the activity and selectivity of zirconia and hafnia-containing tungsten catalysts under similar reaction conditions. Pt-promoted sulfated hafnia (1Pt/HfO_2–SO_4) exhibits much higher activity compared to tungsten-zirconia and tungsten–hafnia catalysts for hydroisomerization of *n*-hexadecane. Cracking is the predominant reaction occurring on sulfated hafnia. In comparison with tungsten-zirconia, tungsten-containing hafnia catalysts have exhibited lower activity for hydroisomerization and, as expected, their selectivity to *i*-C_{16} was nearly ca 85 %. In order to correlate acidity and activity for *n*-hexadecane isomerization, runs were made over three catalysts and a plot of L/B ratio to *n*-hexadecane conversion is shown in Fig. 11. It is better to compare the acidity of catalysts at the same temperature as that as catalyst testing. In this respect, the L/B ratio was taken after desorption of pyridine at 473 K and the values were plotted against *n*-hexadecane conversion for various catalysts. A straight line was obtained and the catalyst having a higher L/B ratio exhibited higher activity for *n*-hexadecane conversion. However, the catalyst possessing more Lewis acid sites contributed more to cracking than to the desired isomerized product. For example, sulfated hafnia (1Pt/HfO_2–SO_4) has shown very high cracking activity (Table 2), accounting for most of the *n*-hexadecane conversion. Although the L/B ratio of tungsten-containing hafnia catalysts are lower as compared to the other two catalysts studied here, the former catalysts exhibit both higher activity and selectivity to *i*-C_{16} for *n*-hexadecane at higher operating temperatures.

In general, isomerization reactions take place over bifunctional catalysts containing metallic sites for hydrogenation/dehydrogenation and acid sites for skeletal isomerization via carbenium ions [27–32]. According to the classical isomerization mechanism, paraffins are dehydrogenated over metal sites of the catalyst, and the

olefins produced migrate to and protonate on the Brønsted acid sites to the corresponding alkylcarbenium ions. These carbenium ions undergo skeletal rearrangement and β-scission. This step is followed by deprotonation and hydrogenation over metal sites to give the corresponding paraffins.

Scheme 1 shows that, depending on the strength of acid sites, the catalyst may either produce isomerized alkanes or cracked products. From the above discussion, HfO_2 based WO_3 catalysts show higher selectivity towards iso-C_{16} compared to sulfated hafnia. This is likely due to the fact that sulfated hafnia is a stronger acid that retains the adsorbed hydrocarbon and this promotes more cracking than isomerization. Also, sulfated hafnia produces more multibranched-C_{16} isomers, which are likely to participate in further cracking via rearrangement and β-scission of carbenium ions. From the lack of methane and ethane in the cracked products, hydrogenolysis on the noble metal is deemed to be a negligible reaction. Therefore, the yields to C_1 and C_2 are not included.

4 Conclusions

In the present study, hydroisomerization of *n*-hexadecane was carried out in a trickle-bed reactor using Pt-promoted tungsten- and sulfate-modified hafnia as catalysts at high pressure and temperatures. XRD analysis of the calcined catalysts show that hafnia exhibits mainly monoclinic and orthorhombic phases while zirconia exhibits a tetragonal phase. The tetragonal form of WO_3 increases with increasing tungsten loading over hafnia. DRIFTS of pyridine adsorption for both catalysts suggests that Lewis acid sites were dominant over Brønsted acid sites even at higher temperatures (473 K). WO_3/HfO_2 catalysts exhibit moderate activity and higher selectivity for isomerization of *n*-hexadecane. It is surprising to see using WO_3/HfO_2 catalysts that the selectivity to iso-C_{16} does not vary with *n*-C_{16} conversion. However, sulfated hafnia is active even at much lower temperature than WO_3/HfO_2 catalysts, but it selectively produces more cracking products, especially C_4–C_8.

Acknowledgments The study was supported by the Commonwealth of Kentucky.

References

1. Meyers RA (1996) Handbook of petroleum refining processes. McGraw-Hill, New York
2. Taylor RJ, Perry RH (1994) Appl Catal A Gen 119:121
3. Ernst S, Weitkamp J, Martens JA, Jacobs PA (1989) Appl Catal A Gen 48:137
4. Weitkamp J (1983) Appl Catal 8:123
5. Molina R, Moreno S, Coelho AV, Martens JA, Jacobs PA, Poncelet G (1994) J Catal 148:304
6. Holm VCF, Bailey GC (1962) US Patent 3,032,599
7. Hino M, Arata K (1987) J Chem Soc Chem Commun 18:1259
8. Hino M, Arata K (1988) In: Proceedings of 9th international congress on catalysis, vol 4, p 1727
9. Iglesia E, Barton DG, Soled SL, Miseo S, Baumgartner JE, Gates WE, Fuentes GA, Meitzner GC (1996) Std Surf Sci Catal 101:533
10. Soled SL, Gates E, Iglesia E. (1995) U.S. Patent 5,422,327
11. Boyse RA, Ko EI (1997) J Catal 171:191
12. Barton DG, Soled SL, Iglesia E (1998) Top Catal 6:87
13. Brei VV (2005) Theor Exp Chem 41:165
14. Iglesia E, Soled SL, Kramer GM (1993) J Catal 144:238
15. Barton DG, Soled SL, Meitzner GD, Fuentes GA, Iglesia E (1999) J Catal 181:57
16. Deldari H (2005) Appl Catal A Gen 293:1
17. Wen MY, Wender I, Tierney JW (1990) Energy Fuels 4:372
18. Keogh RA, Sparks D, Hu J, Wender I, Tierney JW 91994) Energy Fuels 8:755
19. Keogh RA, Davis BH (1999) Catal Lett 57:33
20. Zhang S, Zhang Y, Tierney JW, Wender I (1998) Ind Eng Chem Res 37:2208
21. Zhang S, Zhang Y, Tierney JW, Wender I (2000) Appl Catal A Gen 193:155
22. Martinez A, Prieto G, Arribas MA, Concepcion P (2006) Appl Catal A Gen 309:224
23. Kang J, Lee EC, Chang KJ (2003) Phys Rev B 68:54106
24. Wan KT, Khouw CB, Davis ME (1996) J Catal 158:311
25. Arata K, Hino M (1984) React Kinet Catal Lett 25:143
26. Ahmed MA (2011) Fuel Process Tech 92:1121
27. Weitkamp J (1982) Ind Eng Chem Prod Res Dev 21:550
28. Liu Y, Liu C, Tian A, Lin L (2004) Energy Fuels 18:1266
29. Alvarez F, Ribeiro FR, Perot G, Thomazeau C, Guisnet M (1996) J Catal 162:179
30. Campelo M, Lafont F, Marinas JM (1998) Appl Catal A Gen 170: 139
31. Gigis MJ, Tsao YP (1996) Ind Eng Chem Res 35:386
32. Walendziewski J, Pniak B (2003) Appl Catal A Gen 250:39
33. Park KC, Ihm SK (2001) Appl Catal A Gen 203:201